GEOPHYSICS, VOL. 83, NO. 5 (SEPTEMBER-OCTOBER 2018); P. E347–E356, 7 FIGS.
10.1190/GEO2017-0849.1

An airborne electromagnetic system with a three-component transmitter and three-component receiver capable of detecting extremely conductive bodies

Richard S. Smith[1]

ABSTRACT

Extremely conductive bodies, such as those containing valuable nickel sulfides, have a secondary response that is dominated by an in-phase component, so this secondary response is very difficult to distinguish from the primary field emanating from the transmitter (because by definition they are identical in temporal shape and phase). Hence, an airborne electromagnetic (AEM) system able to identify the response from the extremely conductive bodies in the ground must be able to predict the primary field to identify and measure the secondary response of the extremely conductive body. This is normally done by having a rigid system and bucking out the predicted primary (which will not change significantly due to the rigidity). Unfortunately, these rigid systems must be small and are not capable of detecting extremely conductive bodies buried deeper than approximately 100 m. Another approach is to measure the transmitter current and geometry and subtract the primary mathematically, but these measurements must be extremely accurate and this is difficult or expensive, so it has not been done successfully for an AEM system. I exploit the geometric relationship of the primary fields from a three-component (3C) dipole transmitter. If the transmitter is mathematically rotated so that one axis points to the receiver, then linear combinations of the fields measured by a 3C receiver can be combined in such a way that the primary fields from the transmitter sum to zero and cancel. Alternatively, the measured transmitter current and response could be used to estimate the transmitter-receiver geometry and then to predict and remove the primary field. Any residual must be the secondary coming from a conductive body in the ground. Hence, extremely conductive bodies containing valuable minerals can be found. An AEM system with a 3C transmitter and a 3C receiver should not be too difficult to build.

INTRODUCTION

Electromagnetic (EM) methods are a successful tool used to explore for mineral deposits (Grant and West, 1965; Nabighian, 1991; Fountain, 1998). They can also be deployed for groundwater investigations, environmental investigations (Ward, 1990), and searching for unexploded ordnance (e.g., Billings et al., 2010). An emerging application of EM methods is in agricultural mapping (e.g., Lück and Müller, 2009). In the hydrocarbon industry, EM systems have been used for many years in induction logging tools (see recent papers by Wang et al., 2009; Davydycheva, 2010a, 2010b) and more recently in seafloor controlled-source EM (CSEM) systems (Chave and Cox, 1982; Cheesman et al., 1987, 1988; MacGregor and Sinha, 2000; Ellingsrud et al., 2002; Constable and Srnka, 2007).

A CSEM system has a transmitter and a receiver. In inductive EM systems, the transmitter is a wire loop that carries a time-varying current. Ampere's law tells us that every current has an associated magnetic field radiating in all directions; in the case of the EM transmitter, the field penetrates below the surface, where mineral deposits are located. This field is called the primary field, and it is made to vary as a function of time, so Faraday's law of induction tells us that an electric field will circulate around the primary magnetic field. Ohm's law tells us that an electric field in a conductive medium (such as in the subsurface) results in the flow of an induced

Manuscript received by the Editor 27 December 2017; revised manuscript received 28 May 2018; published ahead of production 22 June 2018; published online 28 August 2018.
[1]Laurentian University, Harquail School of Earth Sciences, Sudbury, Ontario P3E 2C6, Canada. E-mail: rssmith@laurentian.ca.

current, which has an associated magnetic field (Ampere's law again), which in this case is called the secondary field. This secondary can be detected by a receiver that is usually above the surface of the earth. However, the receiver coil also senses the primary field emanating from the transmitter. A timing link from the transmitter to the receiver means that the receiver field can be decomposed into an in-phase component, that by definition is identical in temporal shape and timing (phase) to the primary, and a residual component, known as the out-of-phase or quadrature phase component. EM systems with transmitter current waveforms that vary sinusoidally at one or more fixed frequencies are called frequency-domain systems, whereas those that have waveforms that switch on and off rapidly as a function of time are called time-domain systems. Smith (2001) explains that time- and frequency-domain systems have in-phase and quadrature components.

In this paper, I concentrate on airborne systems, but the principles described here can also apply to ground EM systems (Nabighian, 1991) and semiairborne systems, in which the transmitter or receiver is in the air and the other is on the ground (e.g., Smith et al., 2001). According to Fountain (1998), the earliest airborne systems used one transmitter and one receiver. Some subsequent systems obtained additional information about the geometry of the target using two pairs of transmitters and receivers. The coaxial pair has the transmitter and receiver coils aligned so that each axial dipole direction (or normal vector) is pointed along a common line generally pointing in the direction of flight; the coplanar pair has the transmitter and receiver coils lie in a common plane — generally horizontal (Fraser, 1979). It is also possible to extract geometric information using a single transmitter and multiple component receivers (Fraser, 1972; Annan, 1986; Best and Bremner, 1986; Smith and Keating, 1996). Specifically, Fraser (1972) and Smith and Keating (1996) describe techniques to determine the depth, dip, strike, and offset of conductors using the information from multiple receiver components. Taking this a step further, Hogg (1986) describes a system with a three-component (3C) receiver and two-component (2C) transmitters; he uses model studies to show that the multiple components could be used to infer the geometry of the subsurface conductor.

The ability of these EM systems to detect copper and nickel mineralization (so-called magmatic segregation deposits) is important in mineral exploration because these deposits are valuable. However, these deposits are sometimes extremely conductive, so they have a quadrature response that is too small to measure, but a significantly larger in-phase response, a situation sometimes called the inductive limit (Grant and West, 1965).

Because extremely conductive bodies have a response that is predominantly in-phase, special methods are required to identify this in-phase secondary response in the presence of a strong primary field. One approach is to buck out the primary response, which can be done in two ways. In active bucking, a smaller bucking transmitter coil is placed between the transmitter and receiver and is oriented in such a way that the field from the transmitter bucking coil cancels the primary field from the transmitter at the receiver (Kovacs et al., 1995). This requires that the transmitter and bucking transmitter coil transmit exactly the same waveform and that the distances between, and orientation of, all the coils do not change. Passive bucking is similar, except there is a small receiver bucking coil placed near the transmitter, which when combined with the signal from the receiver will also cancel the primary field (provided once again that the distances between, and orientations of, the coils do not change). These types of systems with rigid geometry, called rigid-boom systems, are generally attached to or towed below helicopters (Fountain, 1998). Rather than rely on time-varying magnetic fields to induce a bucking signal, it is also possible to use an electronic signal from the transmitter (with any appropriate phase shifts) to remove the primary field. This approach also generally assumes that the geometry does not change significantly.

A similar approach is to place or orient the receiver so that it is null coupled with the transmitter and hence will not measure a primary field (Fountain, 1998). Once again, the geometry must be held rigid, so the null coupling is maintained. Hefford (2006) shows that for a system in which the receiver and transmitter were less than 10 m from each other, the geometry variations had to be restricted to less than a millimeter to see a strong in-phase response from a subsurface conductor.

A second approach is to continually monitor the transmitter current and the relative offset and orientation of the transmitter and receiver and then predict the field from the transmitter that would be measured at the receiver. This predicted field can be subtracted from the measured field, and what remains is the secondary field from the extremely good conductor. Hefford (2006) shows that the closer the transmitter is to the receiver, the more accurately the transmitter current and system geometry must be measured. When the transmitter and receiver are a significant distance from each other (e.g., in ground or borehole methods), the primary can be predicted and subtracted successfully (e.g., West et al., 1984; Smith and Balch, 2000). With airborne systems, this has never been done successfully due to the very stringent accuracy requirements.

A third approach (Zandee et al., 1985) suggested crosscorrelating a transient transmitter signal with the received signal to decompose the response into in-phase and quadrature components. This could be done at several frequencies, and the intent was to use the very-low-frequency in-phase signal to correct for the relative motion of the transmitter and receiver. However, using this approach assumes no impact of any secondary field at the lowest frequency, so one potential impact is that the correction will remove the secondary field from an extremely good conductor.

Cartier et al. (1952, 1958) describe a fourth approach using a system with two transmitter and receiver coil pairs, one coaxial and one coplanar, both pairs being separated by the same distance. The primary field measured using the coaxial pair will be twice the magnitude of the primary field measured with the coplanar pair, so when this is not the case, there must be an in-phase secondary field coming from a nearby conductor. This system has the receivers housed in a towed bird a specific distance behind and below the aircraft. The coaxial pair has the receiver dipole pointing toward the corresponding transmitter in the aircraft, which is also pointing in the same direction. The coplanar coil is a vertical coil with its dipole direction being transverse to the direction of flight. For the two primaries to be in a precise ratio of 2:1, the receiver has to be directly behind the aircraft, the aircraft had to be pointing straight down the survey line, and the receiver had to be at the correct angle behind and below the aircraft, so that the coaxial receiver is pointing directly at the transmitter. These criteria are difficult to achieve in practice and were most closely satisfied in calm wind conditions. Cartier et al. (1958) argue that the system was relatively insensitive to the relative position of the transmitter and receiver; despite this, they also suggested that a servo system could rotate the transmitter coils so that the axis of the coaxial transmitter coil

was always pointing toward the receiver. However, to get a true coaxial configuration, the receiver would also have to have a servo system. In the system described in this paper, the transmitter and receiver are comprised of three components and the rotations (or equivalent operations) can be done mathematically rather that physically. Rotation of the receiver is not required because the three components measured can be used to calculate vector quantities, which are independent of the rotation of the receiver coil.

The frequency-domain airborne EM (AEM) systems that use a towed bird are not rigid and are designed to only measure the quadrature component (Pemberton, 1962). The time-domain systems that measure only in the off-time are also essentially only measuring the quadrature field. Even those that measure in the on-time are actually measuring the on-time quadrature field (Smith, 2001). These quadrature systems are unable to identify extremely conductive responses because by definition they have no quadrature response (Smith, 2001). All modern time-domain airborne systems are quadrature systems, so a system capable of detecting extreme conductors is required.

The system described in this paper (and also described in a patent application; Smith [2014]) uses a 3C dipole transmitter and a 3C dipole receiver. The geometric relation of the transmitter to the receiver is not rigid; it is allowed to vary. Nor is it necessary to use independent measurement devices to monitor to great accuracy the transmitter current and the position of the receiver relative to transmitter. However, the new system uses the nature of the fields from the 3C transmitter to remove the primary so as to detect the in-phase secondary fields. In this way, extremely conductive bodies can be detected.

FIELDS OF THE 3C TRANSMITTER SYSTEM

The system uses magnetic dipole transmitters and magnetic dipole receivers. The magnetic field vector $\mathbf{H}(r)$ at a location (x, y, z) from a magnetic dipole at the origin (0, 0, 0) is given by (Billings et al., 2010, after correcting the typographic error)

$$\mathbf{H}(r) = \frac{M}{4\pi r^3}(3(\mathbf{m}' \cdot \mathbf{r}')\mathbf{r}' - \mathbf{m}'), \tag{1}$$

where $r = (x^2 + y^2 + z^2)^{1/2}$ is the scalar distance from the transmitter to the receiver dipole; M is the dipole-moment magnitude of the transmitter; $\mathbf{m}'$ is the unit-vector orientation of the transmitter dipole; and $\mathbf{r}'$ is the unit vector from the dipole to the observation location ($\mathbf{r}' = \mathbf{r}/r$), where $\mathbf{r} = (x, y, z)$. For example, if the transmitter dipole is parallel to the z-axis, then $\mathbf{m}' = (0,0,1)$. In the case when the observation point is aligned along the axis of the transmitter dipole, then $\mathbf{m}' = \mathbf{r}'$ and $\mathbf{m}' \cdot \mathbf{r}' = 1$, so that

$$\mathbf{H}(r) = \frac{M}{4\pi r^3}(2\mathbf{m}'), \tag{2}$$

and the magnetic field is in the $\mathbf{m}'$ direction. In the discussion below, an observation point on the axis of a transmitter dipole is said to lie on the axial vector or is said to be at an axial location (i.e., on the axis of the transmitter).

When the observation point is in the plane that is normal to the dipole orientation and contains the dipole (the normal plane), then $\mathbf{m}'$ and $\mathbf{r}'$ are perpendicular and $\mathbf{m}' \cdot \mathbf{r}' = 0$, so

$$\mathbf{H}(r) = -\frac{M}{4\pi r^3}(\mathbf{m}'), \tag{3}$$

which is also in the $\mathbf{m}'$ direction, but pointing in the opposite (negative) direction. Note that, for similar values of r, the magnitude on the normal plane is half that on the axial vector. When the observation point is away from the axial vector and the normal plane, the orientation of the field is a linear combination of the $\mathbf{m}'$ and $\mathbf{r}'$ directions. Figure 1 shows the magnetic field vectors for a dipole located at the origin and oriented in the z-direction. In order that the more distant vectors can be seen, the lengths of the arrows have been multiplied by $4\pi r^3$. Because the field of a dipole is axially symmetric about the dipole axis, this image can be rotated about the z-axis to create the 3D field. The diagram illustrates that the locations where the field is strictly vertical are only on the axial vector ($x = 0$), where it is pointing up; or on the normal plane ($z = 0$), where it is pointing down (and half the magnitude). At the origin, $r = 0$, so the dipole field is undefined. Away from the axis of the dipole and the normal plane, the dipole field contains a nonzero horizontal component.

For a 3C transmitter, each transmitter is at the same location and pointing in a different direction. Figure 2 shows a 3D view with the transmitter, which for the sake of illustration, can be put at the origin. The three transmitters X, Y, and Z are aligned in the x-, y-, and z-directions, respectively. At a remote location below and to the side of the transmitter at (−10, −10, and −10), there are three fields: fields A, B, and C coming from the X, Y, and Z transmitters. For this remote location, the fields A, B, and C are not orthogonal, but at other remote locations, they could be more or less orthogonal.

Now consider rotation of the transmitter coil set so that one of the transmitter dipole axes has an axial vector that passes through the remote point. For example, if we first rotate the X and Y transmitters 45° around the z-axis toward the y-axis and then rotate the X and Z transmitters around the axial vector of the rotated Y transmitter by 54° to that the Z transmitter rotates down toward the rotated X transmitter axis, then the transmitter is as shown in the upper right corner of Figure 3. This rotated transmitter set is designated X^R Y^R Z^R, with X^R pointing down and away from the viewer, Z^R pointing up and away and parallel to the line that goes from the remote location to the transmitter, and Y^R is still in the horizontal plane but 45° from its previous orientation. Importantly, at the re-

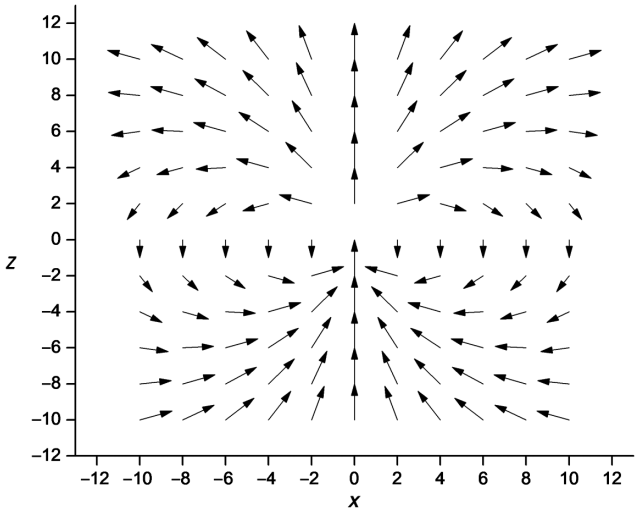

Figure 1. The field of a dipole at the origin directed up the z-axis, so $\mathbf{m}' = (0, 0, 1)$. The magnitude of each vector has been multiplied by $4\pi r^3$ to increase the magnitude of the arrows distant from the dipole.

mote location, the three fields A^R, B^R, and C^R form an orthogonal set (Figure 3). This is because the remote location is now along the axis of the Z^R dipole, so according to equation 2, the field will also be aligned along the axial vector. The X^R and Y^R transmitters are orthogonal to the axial vector and orthogonal to each other. The axial vector for Z^R lies at the intersection of the normal planes of the X^R and Y^R transmitters, so the two fields from these two transmitters at positions along the axis of the Z^R dipole will be antiparallel to their respective transmitter dipole (equation 3) and hence also orthogonal to the axis of Z^R and each other (as is depicted in the bottom left of Figure 3). In the 3D view, C^R is pointing directly up the axial vector toward the transmitter (parallel to Z^R), A^R is pointing up and out of the page (antiparallel to X^R, which is pointing down and into the page), and B^R is horizontal and pointing to the right (antiparallel to Y^R, which is horizontal and pointing to the left).

Because increasing or decreasing the strength of the transmitter will result in a corresponding increase or decrease of the field at the remote location, then the fields at the remote location are linearly proportional to the strengths of the transmitter. Similarly, adding two transmitters at the surface is equivalent to adding the fields of the two transmitters at the remote location. Hence, a linear combination of transmitters will result in the same linear combination of fields at the remote location. Rotation of the transmitter coil set is a linear combination of the unrotated transmitters, so that a linear combination that results in a new transmitter orientation, when applied to the original fields at the remote location, will give the fields of the rotated transmitter coil set. In this way, fields of a 3C transmitter set at a remote location that are not orthogonal can be made orthogonal by a linear transformation of the remote field that is the same linear transformation that would rotate the coil set so that the remote location is on the axial vector of one of the rotated transmitter dipoles. Hence, saying that the transmitter has to be mathematically rotated really means determining the linear transformation required to rotate the transmitter dipoles and then applying this linear transformation to the remote fields (e.g., at the receiver). Note that these arguments apply for any remote location, not just the one depicted in Figures 2 and 3.

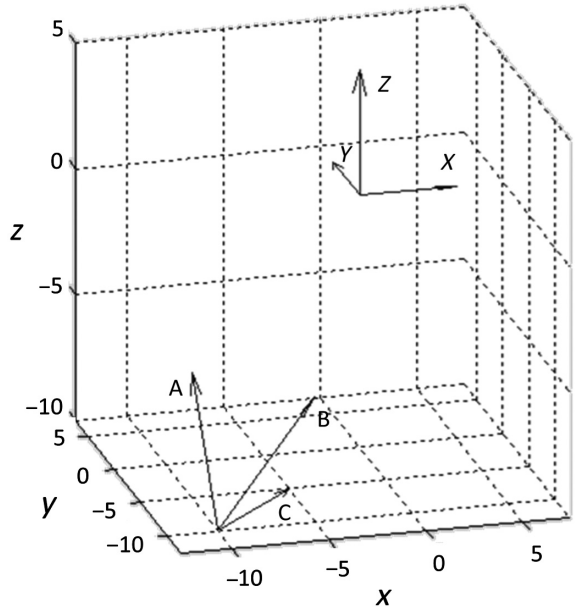

Figure 2. The vector fields at a point (−10, −10, and −10) from a 3C transmitter at the origin. The three transmitter dipoles are oriented in the orthogonal and cardinal (x, y, z) directions, and the fields A, B, and C (in this case not orthogonal) are from the X, Y, and Z transmitters.

DETECTION OF EXTREMELY CONDUCTIVE BODIES

Following the discussion above, the reader can recognize that the three fields from a 3C dipole have unique geometric properties. In the following, I explain how these properties allow the in-phase field from the transmitter to be identified and removed. For example, if the 3C transmitter dipole is rotated so that one transmitter has its axis intersecting the receiver location (as described above), then the three fields from the 3C transmitter will all be orthogonal. The axial primary field will be twice as large as the two transverse fields, and subtracting the sum of the magnitudes of the two transverse fields from the magnitude of the axial field will remove the primary. Note that this property is true all along the axis of the transmitter, so it is not important to know the distance of the transmitter to the receiver. As argued above, the transmitter rotation does not have to be done physically; it can be done mathematically to the fields at the receiver.

To be able to do the mathematical combinations, it is important to be able to identify the magnetic fields $\mathbf{H}_i$ from the ith dipole transmitter and distinguish this from the fields from the other two dipole

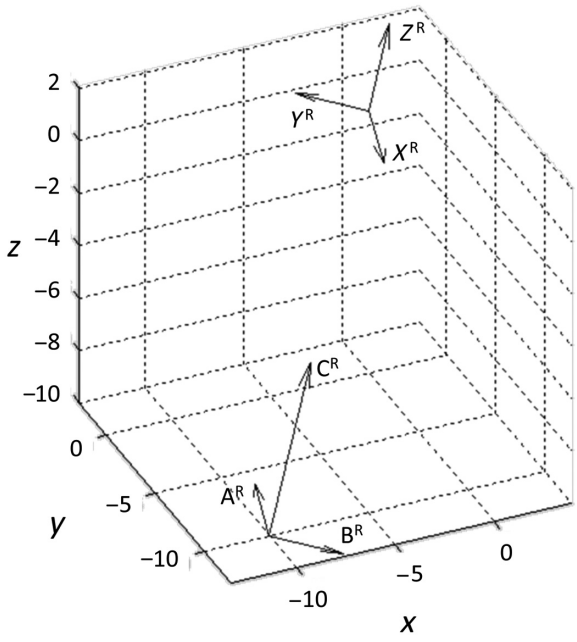

Figure 3. The vectors at the same remote location (−10, −10, and −10) when the 3C transmitter is rotated, so that one dipole (in this case the Z^R dipole) is aligned with the vector joining the remote point to the transmitter. The dipole along the rotated z-axis (Z^R) has a field (C^R) that is coaxial (also points along the axial vector). The rotated x dipole transmitter (X^R), now pointing down and in, has a field (A^R) that is antiparallel (pointing up and out); and the rotated y dipole transmitter (Y^R), now pointing left and is horizontal, has a field (B^R) that is antiparallel, pointing right and is horizontal. Hence, (A^R, B^R, C^R) form an orthogonal set.

transmitters. Practically, this can be done by time interleaving the transmitters or by giving each field a separate and characteristic frequency or base frequency. When rotating these fields mathematically, they will be added and subtracted, so they should be at identical or at least at very similar frequencies. This change to another frequency can be achieved by interpolation between frequencies, which will be discussed in more detail later.

Below I outline two methods that can be used to process the measured data, so as to exploit the geometric properties of fields from a 3C transmitter dipole, with the first method being discussed in more detail.

Method 1: Some vector quantities are independent of the coordinate system, so they will be independent of the orientation of the receiver (as its coordinate system rotates with the receiver). For example, the following quantities are invariant under a change of coordinate system: the dot products of two fields $\mathbf{H}_i \cdot \mathbf{H}_j$, the magnitude of the cross product of two fields $|\mathbf{H}_i \times \mathbf{H}_j|$, and the scalar triple product of three fields $\mathbf{H}_i \cdot (\mathbf{H}_j \times \mathbf{H}_k)$. For the 3C receiver, the formulas for these quantities are

$$\mathbf{H}_x \cdot \mathbf{H}_x = \frac{M_x M_x}{(4\pi r^3)^2}\left(\frac{3x^2}{r^2}+1\right), \tag{4}$$

$$\mathbf{H}_x \cdot \mathbf{H}_y = \frac{M_x M_y}{(4\pi r^3)^2}\left(\frac{3xy}{r^2}\right), \tag{5}$$

$$\mathbf{H}_x \cdot \mathbf{H}_z = \frac{M_x M_z}{(4\pi r^3)^2}\left(\frac{3xz}{r^2}\right), \tag{6}$$

$$\mathbf{H}_y \cdot \mathbf{H}_y = \frac{M_y M_y}{(4\pi r^3)^2}\left(\frac{3y^2}{r^2}+1\right), \tag{7}$$

$$\mathbf{H}_y \cdot \mathbf{H}_z = \frac{M_y M_z}{(4\pi r^3)^2}\left(\frac{3yz}{r^2}\right), \tag{8}$$

$$\mathbf{H}_z \cdot \mathbf{H}_z = \frac{M_z M_z}{(4\pi r^3)^2}\left(\frac{3z^2}{r^2}+1\right), \tag{9}$$

$$\mathbf{H}_x \cdot (\mathbf{H}_y \times \mathbf{H}_z) = \frac{2M_x M_y M_z}{(4\pi r^3)^3}, \tag{10}$$

$$|\mathbf{H}_x \times \mathbf{H}_y| = \frac{M_x M_y}{r(4\pi r^3)^2}\sqrt{4x^2+4y^2+z^2}, \tag{11}$$

$$|\mathbf{H}_x \times \mathbf{H}_z| = \frac{M_x M_z}{r(4\pi r^3)^2}\sqrt{4x^2+y^2+4z^2}, \tag{12}$$

$$|\mathbf{H}_y \times \mathbf{H}_z| = \frac{M_y M_z}{r(4\pi r^3)^2}\sqrt{x^2+4y^2+4z^2}. \tag{13}$$

The invariants on the left side can be measured as can the three moments of each of the transmitters M_x, M_y, and M_z so the only unknowns are x, y, and z. Because there are 10 equations and three unknowns, there are multiple methods to find the unknowns. One simple method involves using equation 10 to estimate $r = \sqrt{x^2+y^2+z^2}$, and then equations 4, 7, and 9 can be used to estimate x, y, and z, respectively, giving the offset of the receiver from the transmitter, $\mathbf{r} = (x, y, z)$. An example of another method is to use nonlinear inversion techniques. Once this offset vector $\mathbf{r}$ is known, then so too is the axial direction, so the transmitter orientation can be rotated so that one transmitter (say the z-directed transmitter) is aligned along the axial direction. In the coordinate frame of the rotated transmitter the receiver location is now $\mathbf{r} = (0,0,r)$ and the above equations become

$$\mathbf{H}_x^R \cdot \mathbf{H}_x^R = \frac{M_x M_x}{(4\pi r^3)^2}, \tag{14}$$

$$\mathbf{H}_x^R \cdot \mathbf{H}_y^R = 0, \tag{15}$$

$$\mathbf{H}_x^R \cdot \mathbf{H}_z^R = 0, \tag{16}$$

$$\mathbf{H}_y^R \cdot \mathbf{H}_y^R = \frac{M_y M_y}{(4\pi r^3)^2}, \tag{17}$$

$$\mathbf{H}_y^R \cdot \mathbf{H}_z^R = 0, \tag{18}$$

$$\mathbf{H}_z^R \cdot \mathbf{H}_z^R = \frac{4M_z M_z}{(4\pi r^3)^2}, \tag{19}$$

$$\mathbf{H}_x^R \cdot (\mathbf{H}_y^R \times \mathbf{H}_z^R) = \frac{2M_x M_y M_z}{(4\pi r^3)^3}, \tag{20}$$

$$|\mathbf{H}_x^R \times \mathbf{H}_y^R| = \frac{M_x M_y}{(4\pi r^3)^2}, \tag{21}$$

$$|\mathbf{H}_x^R \times \mathbf{H}_z^R| = \frac{2M_x M_z}{(4\pi r^3)^2}, \tag{22}$$

$$|\mathbf{H}_y^R \times \mathbf{H}_z^R| = \frac{2M_y M_z}{(4\pi r^3)^2}, \tag{23}$$

where the magnetic fields on the left are the fields from the rotated transmitter, but they are obtained by the equivalent linear transfor-

mation of the receiver fields. When these 10 invariants are recalculated, the cross terms of the dot products (equations 15, 16, and 18) should all be zero if there is only a primary field present. If the cross dot products are not zero, then this implies that there is a nearby conductor with an in-phase secondary field response.

Furthermore, the relative sizes of each of the nonzero terms are known, and these can be combined in ways that should also be zero if there is no conductor with an in-phase component present. Substituting equations 14, 17, 19–23 into the formulas on the left of equations 24–31, it is possible to verify that all these combinations give a zero result (the R superscipt has been dropped for simplicity):

$$2|\mathbf{H}_x \times \mathbf{H}_y| - \frac{M_y}{M_z}|\mathbf{H}_x \times \mathbf{H}_z| = 0, \tag{24}$$

$$2|\mathbf{H}_x \times \mathbf{H}_y| - \frac{M_x}{M_z}|\mathbf{H}_y \times \mathbf{H}_z| = 0, \tag{25}$$

$$|\mathbf{H}_x \times \mathbf{H}_z| - \frac{M_x}{M_y}|\mathbf{H}_y \times \mathbf{H}_z| = 0, \tag{26}$$

$$4|\mathbf{H}_x \times \mathbf{H}_y| - \frac{M_y}{M_z}|\mathbf{H}_x \times \mathbf{H}_z| - \frac{M_x}{M_z}|\mathbf{H}_y \times \mathbf{H}_z| = 0, \tag{27}$$

$$4\mathbf{H}_x \cdot \mathbf{H}_x - \frac{M_x^2}{M_z^2}\mathbf{H}_z \cdot \mathbf{H}_z = 0, \tag{28}$$

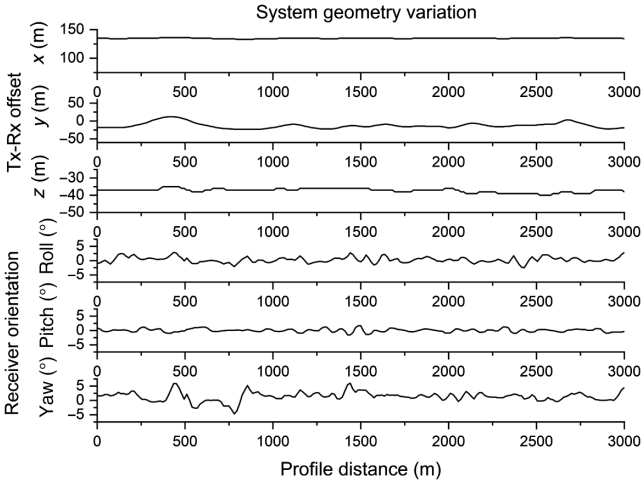

Figure 4. The changing geometric relationship between a 3C transmitter and a 3C receiver as a function of distance along a profile. The offset of the receiver from the transmitter is given by the x, y, and z values, and the orientation of the receiver is defined by the roll, pitch, and yaw in the bottom three panels. The mean position of the bird is $x = 126$ m behind the aircraft, $z = -33$ m below the aircraft, and $y = -11$ m to the port of the aircraft.

$$4\mathbf{H}_y \cdot \mathbf{H}_y - \frac{M_y^2}{M_z^2}\mathbf{H}_z \cdot \mathbf{H}_z = 0, \tag{29}$$

$$\mathbf{H}_x \cdot \mathbf{H}_x - \frac{M_x^2}{M_y^2}\mathbf{H}_y \cdot \mathbf{H}_y = 0, \tag{30}$$

$$\mathbf{H}_z \cdot \mathbf{H}_z - 2\frac{M_z^2}{M_x^2}\mathbf{H}_x \cdot \mathbf{H}_x - 2\frac{M_z^2}{M_y^2}\mathbf{H}_y \cdot \mathbf{H}_y = 0. \tag{31}$$

With some imagination, other combinations could also be constructed that sum to zero.

In procedures described above, I have assumed that the in-phase secondary field from the conductor does not distort the estimates of r and x, y, and z. This assumption is justified for the case of an AEM system by generating a synthetic example and showing that a subsurface conductor can be identified satisfactorily. The transmitter is a 3C transmitter, and the x, y, and z offsets of the receiver (Rx) from the transmitter (Tx) (shown in Figure 4) are varying along the profile. The bottom three panels of Figure 4 show changes in the orientation of the receiver coil as it moves along the profile. These geometric variations are realistic, having been estimated from field data collected using a real fixed-wing system. The transmitter is assumed to have its z-axis oriented vertically. This is not a limiting assumption because a nonvertical z transmitter is equivalent to a different x, y, and z offset. (For a real-data example, the z-direction will be defined relative to the transmitter and the z-direction will rotate as the transmitter rotates. All offsets would then be estimated in the transmitter frame of references.) The synthetic primary field at each (rotating) receiver coil was then calculated at each location. Also, the secondary field from a sphere of radius 50 m that is buried 50 m below the ground surface at profile location 1500 m was calculated and added to the primary field. The rotational invariant dot products were then calculated and plotted in Figure 5. The spatial changes in the invariants along the profile have a wavelength comparable with the (x, y, z) changes in the transmitter-receiver offset (the strongest correlation seems to be with the y offset). There are no variations in the invariants that have a similar wavelength to the receiver roll, pitch, or yaw, which is consistent with the invariants being independent of the orientation of the receiver. More importantly, there is no response evident near 1500 m on the profile (the conductor location), so the small secondary that has been added is clearly so small as to be obscured by the large primary-field variations associated with changes in the system geometry. The values of the invariants at each location of the profile in Figure 5 were then used to estimate the offsets x, y, and z using a nonlinear inversion routine. Then, the linear transformation (comprising a set of trigonometric rotations) that would rotate the 3C transmitter in its frame of reference so that the axial vector passes through the receiver was determined. This transformation was applied to the original primary (plus secondary fields) measured at the receiver, and the invariants calculated from these are shown in Figure 6. Note that the dot products $\mathbf{H}_i^R \cdot \mathbf{H}_j^R$ for the cases when $i \neq j$ are zero away from the conductor and are anomalous (nonzero) close to the conductor at location 1500 m. The amplitude of the secondary evident in Figure 6 is more than two orders of magnitude smaller than the corresponding primary (plus the much smaller secondary) in Figure 5. This

shows that the impact of the in-phase secondary is small enough that it has not corrupted the estimate of the receiver position relative to the transmitter, so that the primary can be essentially removed.

The dot products $\mathbf{H}_i^R \cdot \mathbf{H}_i^R$ for $i = x, y, z$ are not zero; their magnitude is a function of r and the dipole moments (equations 14, 17, and 19). However, linear combinations of these terms (for example, equations 28 and 29) become zero when there are no conductors present and are nonzero close to a conductor (Figure 7). Hence, I conclude that although the secondary field from the conductor is slightly distorting the estimates of the offsets x, y, and z, these estimates are sufficiently accurate that the secondary is not hindering the ability of the procedure described to identify a unknown conductor in the subsurface.

If the above procedures are applied to the in-phase components of the response and an anomalous response is identified, then there is a conductive body in the subsurface. If there is no corresponding anomaly on the quadrature component, then the conductive body can be clearly identified as an extremely conductive body.

Method 2: The nine measured components could be inverted using a nonlinear iterative method to estimate the relative position and orientation of the receiver with respect to the transmitter. Once again, this assumes that there is no secondary in-phase response, but because I have used the nonlinear inversion in the implementation of method 1, and it had no adverse impact there, it should have no adverse impact in method 2. Using the estimated geometry and the measured dipole moments, the primary fields could be calculated. If there is a nonzero secondary in-phase response, it is extremely unlikely that all nine components of the calculated primary will be equal to those measured (because the secondary field will be coming from the subsurface and will have a different shape at the receiver to the shape of the primary fields). Hence, a significant discrepancy will be indicative of a secondary in-phase response and hence a conductive body in the subsurface.

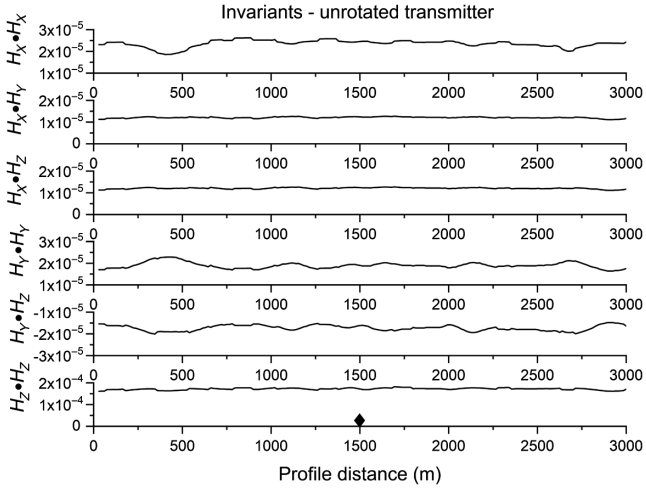

Figure 5. The rotational invariants of the primary plus secondary field (from the transmitter and the anomalous body) at the receiver. In this case, the transmitter is oriented vertically. Most of the variation observed in the rotational invariants is due to changes in the x, y, and z offset. The invariants have units of $(\mathrm{A/m})^2$. There is no obvious response at the location of the conductor (marked with a diamond at 1500 m).

PRACTICAL IMPLEMENTATION

To implement a system such as described above, we need a system with three transmitters that can be clearly distinguished from each other. An approach used by the ALLTEM system (Wright et al., 2007) is to multiplex or interleave the waveforms in the time domain, which means transmitting from each transmitter in turn, whereas the other two transmitters are switched off. This would take three times longer than when using a single transmitter. A faster

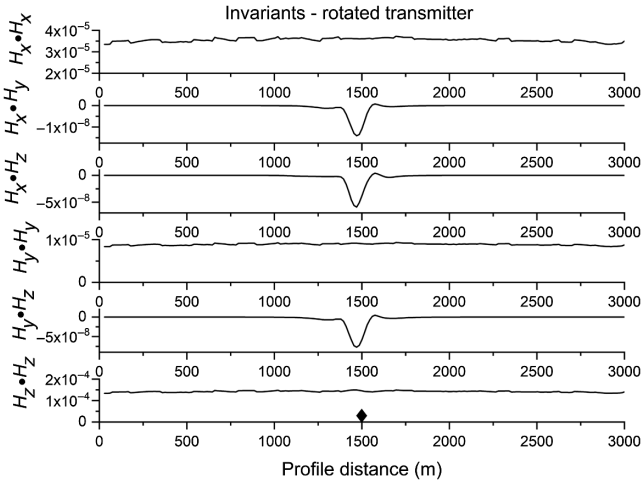

Figure 6. The rotational invariants of the total field (from the transmitter and the anomalous body) at the receiver. In this case, effectively the transmitter is rotated so that its z-axis is oriented along the vector pointing from the transmitter to the receiver. When $i \neq j$, the $\mathbf{H}_i^R \cdot \mathbf{H}_j^R$ terms are zero, except where there is a secondary response, in which case, the term shows a nonzero anomalous response at the location of the conductor (marked with a diamond at 1500 m). In the case when the two vectors in the dot product are the same ($i = j$), there is not an anomalous response and the resultant is more than two orders of magnitude larger. The invariants have units of $(\mathrm{A/m})^2$.

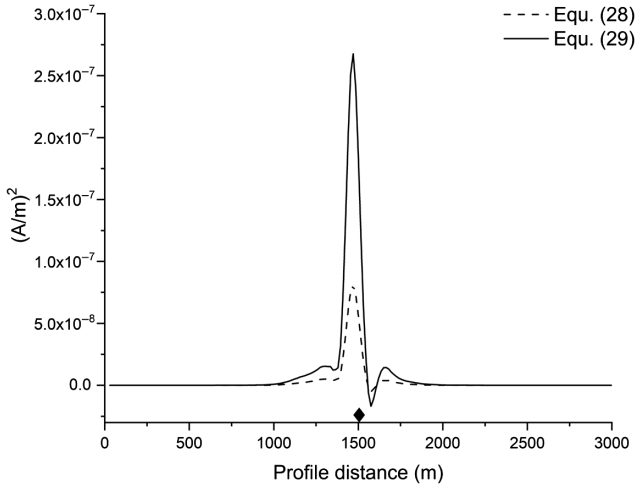

Figure 7. Equations 28 and 29 involving combinations of the $\mathbf{H}_i^R \cdot \mathbf{H}_i^R$ terms. The combinations now have a zero response away from the conductor and an anomalous response at the conductor (marked with a diamond at 1500 m).

option is to transmit the waveforms at base frequencies, which have harmonics that interleave (e.g., a triplet of base frequencies at 1, 2, and 4 Hz has sets of harmonics at the following frequencies 3, 5, 7, ... Hz; 6, 10, 14, ... Hz; and 12, 20, 28, ... Hz, so there is no overlap). In practice, a set of frequencies that does not have any harmonics at power-line frequencies would be chosen. In North America, where the power-line frequency is 60 Hz, this could be 7.5, 15, and 30 Hz, for example, which are frequencies that are obtainable with reasonable noise levels for late-time quadrature data (Konieczny et al., 2016), so they should be adequate for on-time in-phase data because the amplitudes of the latter type of data are much larger. This interleaving procedure would allow the data to be collected three times faster, but the disadvantage is that to combine the results from the individual transmitter dipoles, it would be necessary to interpolate the data from all transmitters to a common frequency (or set of frequencies) so that linear combinations of the data from each transmitter could be used to create a rotated transmitter set at the desired frequency or frequencies.

If the subsurface conductor is extremely conductive, then the response at the inductive limit is independent of frequency, so interpolation would not be required. In this circumstance, the interpolation is only important for quadrature data, but quadrature data do not have to be added; it can be left at separate base frequencies and interpreted independently. For the case in which the subsurface conductor is not extremely conductive, the frequencies might have to be close together. One way this can be done is to operate each transmitter with a sinusoidal waveform at a slightly different frequency, say, 29, 30, and 31 Hz. A hybrid approach would be to operate one principal transmitter (say the z-component) with a time-domain waveform at a frequency such as 30 Hz and the other two transmitters have sinusoidal waveforms at different frequencies. These sinusoidal waveforms will have minimal harmonics and not interfere with off-time (quadrature) data associated with the principal transmitter.

In the discussion above, orthogonal dipoles are assumed; however, strict orthogonality is not critical. In the same way that a linear combination can be used to rotate a transmitter, a linear combination of near-orthogonal transmitters can be used to mathematically construct a virtual orthogonal set. Practically, a rigid 3C transmitter set could be constructed, attempting to make it as orthogonal as possible, but any nonorthogonality could be corrected with a specific linear combination determined as part of a calibration procedure. The changes generated as a result of a change in the geometry of the structure of the coil set could be corrected by periodically recalibrating the orthogonality of the coil set.

The requirement for dipole transmitters is not necessarily that stringent. Large loops are not strictly dipoles, but at sufficiently large distances from the transmitter, they have fields that are essentially dipolar in their geometric character. Hence, if the receiver is a distance from the transmitter that is approximately 5−10 times the radius of the transmitter loop, then the field of the transmitter at the receiver can be very well-approximated by a dipole field.

The 3C receivers have been used on the Dighem I system (Fraser 1972) and the GEOTEM, MEGATEM, and HeliGEOTEM systems (Smith and Keating, 1996; Smith et al., 2009). However, a 3C transmitter is a new concept for airborne EM. A prototype helicopter system with a 2C transmitter was built and tested by Aerodat in the 1980s (Hogg, 1986). This type of system could be extended to three components with a 50% increase in weight. A 3C transmitter could also be built on a fixed-wing system. The typical transmitter is a horizontal loop (essentially a vertical dipole). A transverse dipole transmitter was used on the Stanmac system (Fountain, 1998) with the wire running from nose to tail along the bottom of the fuselage and then back along the top of the fuselage. This was a very early system that was mounted on an old wooden aircraft, but the 1969 versions of the INCO system had a similar transverse transmitter. The loop was above the fuselage of a DHC-6 Twin Otter, with its top edge running from the highest part of the vertical stabilizer forward toward the cockpit and then down and back to the stabilizer to close the loop. A longitudinal dipole transmitter would require a wire that runs above and out along the length of the wing and then down below the bottom of the fuselage. An alternate arrangement would be to have one or more small loops at the front and or back of the aircraft, such as the TRIDEM system (specifically the Canso installation) or the EM-30 system (Fountain, 1998).

The variables M_x, M_y, and M_z in the above formulation means that the dipole moments need not be identical or even similar; they may even differ by a significant amount. Of course the 3C transmitter could also be on a blimp, an airship, a balloon, or attached to a structure on the ground. The receivers could be towed by or attached to the aircraft. The aircraft could be manned or unmanned. The practical implementation of this system is the next challenge, but it should be feasible.

DATA INTEPRETATION

Once a system has been built and data have been collected, techniques will have to be developed for processing and interpreting the data. One approach is to take synthetic data and calculate the vector invariants and combinations thereof after the transmitter has been rotated (e.g., equations 15, 16, 18, and 24–31). The resultant profiles of the rotated invariants can be examined to look for features that would assist in the interpretation. For example, the relative sizes of peaks and troughs and the distances between these peaks and troughs could be used to estimate the dip, strike, and depth of the subsurface conductor. Alternatively, the synthetic invariant profiles could be fit to the corresponding measured data by manually or automatically adjusting the model until the data are explained.

A second approach could be to use the nine components measured to estimate the orientation of the receiver and possibly the transmitter and then to rotate the measured data to some nominal geometry, for example, where the transmitters and receivers have their dipoles aligned with a specific coordinate system (e.g., along line, crossline and up; north, east and up; or aligned with the specific geology). The nominal geometry data could then be compared with synthetic data via forward or inverse modeling after the modeling algorithms have been adapted to handle 3C transmitters. Methods for interpreting 3C transmitter and receiver data have already been described by Desmarais and Smith (2016), whereas those developed for 1C transmitters and 3C receivers (Desmarais and Smith, 2015) could be augmented to handle 3C transmitters. When the response is purely in-phase, it is not possible to estimate the value of the conductivity or conductance (beyond the fact that it is extremely conductive at the base frequency used), but it is possible to use the shape of the profiles to interpret the depth, dip, strike, plunge, thickness, etc. In a case in which there is a quadrature response, then this is not obscured or swamped by the primary, and hence the standard off-time or on-time quadrature methods can be used to interpret the data (e.g., Smith and Keating, 1996; Desmarais

and Smith, 2016). All additional information provided by the nine components might also help to identify where two neighboring conductors are creating a complex interference anomaly.

The issue of dealing with conductive overburden and variations in the topography of conductive overburden will be an issue. It might be that the geometric properties of the secondary fields from the flow of current in the overburden can be approximated by image dipoles in the subsurface (as has been demonstrated by Macnae et al., 1991). The overburden response could be removed in the same way that the field from the primary dipoles is removed. When the overburden is flat, the image dipole would be directly below the transmitter and retreating away from the transmitter, but when there is topography, the image and the direction of retreat would be at an angle dictated by the slope of the topography. In a case in which the overburden is extremely conductive, the image dipole would have a zero velocity.

There is clearly considerable scope for a great deal of future research into processing and interpreting data from 3C transmitter systems.

DISCUSSION

The methods described in this paper are extremely useful for fixed-wing and helicopter time-domain airborne EM systems because these systems are all currently blind to extremely conductive bodies. If the system was deployed on the ground or in boreholes, then the system would have the same capabilities, but the benefits would not be as great because ground systems typically have large offsets between the transmitters and receivers that are comparable with the distances from the conductors. In these cases, the in-phase secondary is comparable in magnitude with the primary. Thus, existing and cheap methods for measuring the system geometry such as differential GPS and drillhole trajectory surveys can be used to satisfactorily predict and subtract the primary field and reveal a secondary in-phase response from an extreme conductor. In the airborne case, the receivers are typically closer to the transmitter than the extreme conductor, so estimating the transmitter current and system geometry accurately is problematic and removing the very large primary is difficult. Hence, carrying two extra transmitters has great benefit for an airborne system but is of less benefit for a ground system.

The system and methodology described in this paper can also be applied to explore for conductors that are not extremely conductive. The benefits are that the relative size of the in-phase and quadrature can be used to more accurately estimate the conductivity. If a survey is being flown in an area where there could be extreme conductors, then the 3C transmitter system will find and identify these as extreme conductors, and it will also find and characterize the poorer conductors. However, existing quadrature systems will only show a weak response from a conductor that is almost an extreme conductor and will not identify them as extreme conductors of economic interest. One example of this is the extremely rich Ovoid deposit at Voisey Bay, which was only identified as a moderate conductor on the quadrature GEOTEM data (Balch, 1999).

CONCLUSION

The airborne EM system described in this paper is capable of identifying the response from extremely conductive bodies. The system requires a 3C transmitter and a 3C receiver. The system is not rigid, so the geometry of the transmitter and receiver can vary, but the nine independent responses measured with this configuration can be used to determine the position of the receiver with respect to the transmitter. This is also possible using rotational invariants, so it is not necessary to determine the orientation of the receiver (although determining the orientation is possible).

Once the geometry of the transmitter and receiver are known, then one method of processing the data is to define specific linear combinations of the fields such that when these combinations are applied, the primary field will sum to zero. If there is no extremely conductive body present, then the in-phase response is comprised only of the primary, so the specific linear combinations of the in-phase response will also sum to zero. In the case in which there is an extremely conductive body present, then this body will have a secondary in-phase response that adds to the primary. This secondary does not significantly corrupt the estimate of the position of the receiver, and the specific linear combinations for that resultant position still show a significant cancellation of the primary field, but not the secondary field. An in-phase profile flown over an extremely conductive body should show a zero away from the conductor and a nonzero response close to the conductor in the linear combination.

Another method of processing the data is to use the estimated geometry to calculate the primary and subtract this from the measured response to give the response of a conductor.

I have argued that the system should not be too difficult to implement and that interpretation procedures can be developed for the data generated by the system.

ACKNOWLEDGMENTS

The patents and patent applications entitled "Multicomponent electromagnetic prospecting apparatus and method of use thereof" also have the following associated numbers: US application number 61/469,931 and 14/005,628, US publication number 2014/0012505 Al, WO2012/129654 A1 (PCT/CA2012/000272, AU2015249137, and CA2,829,817). These patents (and applications) are assigned to Laurentian University and are currently licensed to CGG. Work on this development project was funded by an Industrial Research Chair funded by NSERC, Vale, Glencore, KGHM International, Wallbridge Mining, and the Centre for Excellence in Mining Innovation (CEMI).

DATA AND MATERIALS AVAILABILITY

Data associated with this research are confidential and cannot be released.

REFERENCES

Annan, A. P., 1986, Development of the PROSPECT I airborne electromagnetic system, *in* G. J. Palacky, ed., Airborne resistivity mapping: Geological Survey of Canada Paper 86-22, 63–70.

Balch, S. J., 1999, Geophysics in mineral exploration: Fundamentals and case histories Ni-Cu sulphide deposits with examples from Voisey's Bay, *in* C. Lowe, M. D. Thomas, and W. A. Morris, eds., Geological Association of Canada Short Course Notes 14, 21.

Best, M. E., and T. G. T. Bremner, 1986, The SWEEPEM airborne electromagnetic system, *in* G. J. Palacky, ed., Airborne resistivity mapping: Geological Survey of Canada Paper 86-22, 71–77.

Billings, S. D., L. R. Pasion, L. Beran, N. Lhomme, L.-P. Song, D. W. Oldenburg, K. Kingdon, D. Sinex, and J. Jacobson, 2010, Unexploded ordnance discrimination using magnetic and electromagnetic sensors: Case study from a former military site: Geophysics, **75**, no. 3, B103–B114, doi: 10.1190/1.3377009.

Cartier, W. O., G. H. McLaughlin, W. A. Robinson, and E. M. Wise, 1952, System of airborne conductor measurements: U.S. Patent 2,623,924.
Cartier, W. O., G. H. Mclaughlin, E. M. Wise, and W. A. Robinson, 1958, System of airborne conductor measurements: Canadian Patent 564,361.
Chave, A. D., and C. S. Cox, 1982, Controlled electromagnetic sources for measuring electrical conductivity beneath the oceans. 1: Forward problem and model study: Journal of Geophysical Research, **87**, 5327–5338, doi: 10.1029/JB087iB07p05327.
Cheesman, S. J., R. N. Edwards, and A. D. Chave, 1987, On the theory of sea-floor conductivity mapping using transient electromagnetic systems: Geophysics, **52**, 204–217, doi: 10.1190/1.1442296.
Cheesman, S. J., R. N. Edwards, and L. K. Law, 1988, First results of a new short baseline sea floor transient EM system: 58th Annual International Meeting, SEG, Expanded Abstracts, 259–261, doi: 10.1190/1.1892241.
Constable, S., and L. J. Srnka, 2007, An introduction to marine controlled-source electromagnetic methods for hydrocarbon exploration: Geophysics, **72**, no. 2, WA3–WA12, doi: 10.1190/1.2432483.
Davydycheva, S., 2010a, Separation of azimuthal effects for new-generation resistivity logging tools. Part I: Geophysics, **75**, no. 1, E31–E40, doi: 10.1190/1.3269974.
Davydycheva, S., 2010b, 3D modeling of new-generation (1999-2010) resistivity logging tools: The Leading Edge, **29**, 780–789, doi: 10.1190/1.3462778.
Desmarais, J. K., and R. S. Smith, 2015, Decomposing the electromagnetic response of magnetic dipoles to determine the geometric parameters of a dipole conductor: Exploration Geophysics, **47**, 13–23, doi: 10.1071/EG14070.
Desmarais, J. K., and R. S. Smith, 2016, Benefits of using multi-component transmitter-receiver systems for determining geometrical parameters of a dipole conductor from single-line anomalies: Exploration Geophysics, **47**, 1–12, doi: 10.1071/EG14076.
Ellingsrud, S., T. Eidesmo, S. Johansen, M. C. Sinha, L. M. MacGregor, and S. Constable, 2002, Remote sensing of hydrocarbon layers by seabed logging (SBL): Results from a cruise offshore Angola: The Leading Edge, **21**, 972–982, doi: 10.1190/1.1518433.
Fountain, D. K., 1998, Airborne electromagnetic systems: 50 years of development: Exploration Geophysics, **29**, 1–11, doi: 10.1071/EG998001.
Fraser, D. C., 1972, A new multicoil aerial electromagnetic prospecting system: Geophysics, **37**, 518–537, doi: 10.1190/1.1440277.
Fraser, D. C., 1979, The multicoil II airborne electromagnetic system: Geophysics, **44**, 1367–1394, doi: 10.1190/1.1441013.
Grant, F. S., and G. F. West, 1965, Interpretation theory in applied geophysics: McGraw-Hill.
Hefford, S. W., 2006, Quantifying the effects of transmitter-receiver geometry variations on the capabilities of airborne electromagnetic survey systems to detect targets of high conductance: M.S. thesis, Carleton University.
Hogg, R. L. S., 1986, The Aerodat multigeometry, broadband transient helicopter electromagnetic system, *in* G. J. Palacky, ed., Airborne resistivity mapping: Geological Survey of Canada Paper 86-22, 79–89.
Konieczny, G., A. Smiarowski, and P. Miles, 2016, Breaking through the 25/30 Hz barrier: Lowering the base frequency of the HELITEM airborne EM system: 86th Annual International Meeting, SEG, Expanded Abstracts, 2218–2222, doi: 10.1190/segam2016-13957502.1.
Kovacs, A., J. Holladay, and C. Bergeron Jr., 1995, The footprint/altitude ratio for helicopter electromagnetic sounding of sea-ice thickness: Comparison of theoretical and field estimates: Geophysics, **60**, 374–380, doi: 10.1190/1.1443773.
Lück, E., and M. Müller, 2009, Forward to special issue: Near Surface Geophysics, **7**, 3, doi: 10.3997/1873-0604.2008037.
MacGregor, L. M., and M. C. Sinha, 2000, Use of marine controlled source electromagnetic sounding for sub-basalt exploration: Geophysical Prospecting, **48**, 1091–1106, doi: 10.1046/j.1365-2478.2000.00227.x.
Macnae, J. C., R. Smith, B. D. Polzer, Y. Lamontagne, and P. S. Klinkert, 1991, Conductivity-depth imaging of airborne electromagnetic step-response data: Geophysics, **56**, 102–114, doi: 10.1190/1.1442945.
Nabighian, M. N., 1991, Electromagnetic methods in applied geophysics, vol. 2: Applications, part A and B: SEG.
Pemberton, R., 1962, Airborne electromagnetics in review: Geophysics, **27**, 691–713, doi: 10.1190/1.1439081.
Smith, R. S., 2001, On removing the primary field from fixed-wing time-domain airborne electromagnetic data: Some consequences for quantitative modeling, estimating bird position and detecting perfect conductors: Geophysical Prospecting, **49**, 405–416, doi: 10.1046/j.1365-2478.2001.00266.x.
Smith, R. S., 2014, Multi-component electromagnetic prospecting apparatus and method of use thereof: U.S. Patent US 2014/0012505 Al.
Smith, R. S., A. P. Annan, and P. D. McGowan, 2001, A comparison of data from airborne, semi-airborne and ground electromagnetic systems: Geophysics, **66**, 1379–1385, doi: 10.1190/1.1487084.
Smith, R. S., and S. J. Balch, 2000, Robust estimation of the in-phase response from impulse-response TEM measurements taken during the transmitter switch-off and the transmitter off time: Theory and an example from Voisey's Bay: Geophysics, **65**, 476–481, doi: 10.1190/1.1444741.
Smith, R. S., G. Hodges, and J. Lemieux, 2009, Case histories illustrating the characteristics of the HeliGEOTEM system: Exploration Geophysics, **40**, 246–256, doi: 10.1071/EG09006.
Smith, R. S., and P. B. Keating, 1996, The usefulness of multicomponent, time-domain airborne electromagnetic measurements: Geophysics, **61**, 74–81, doi: 10.1190/1.1443958.
Wang, G. L., C. Torres-Verdín, and S. Gianzero, 2009, Fast simulation of triaxial borehole induction measurements acquired in axially symmetrical and transversely isotropic media: Geophysics, **74**, no. 6, E233–E249, doi: 10.1190/1.3261745.
Ward, S. H., 1990, Geotechnical and environmental geophysics: SEG.
West, G. F., J. C. Macnae, and Y. Lamontagne, 1984, A time-domain electromagnetic system measuring the step response of the ground: Geophysics, **49**, 1010–1026, doi: 10.1190/1.1441716.
Wright, D. L., C. W. Moulton, T. H. Asch, P. J. Brown, M. N. Nabighian, Y. Li, and C. P. Oden, 2007, ALLTEM UXO detection sensitivity and inversions for target parameters from Yuma proving ground test data: Proceedings of the Symposium on the Application of Geophysics to Engineering and Environmental Problems, 1422–1435.
Zandee, A. P., M. E. Best, and T. G. T. Bremner, 1985, Sweepem, a new airborne electromagnetic system: 55th Annual International Meeting, SEG, Expanded Abstracts, 236–239, doi: 10.1190/1.1892701.